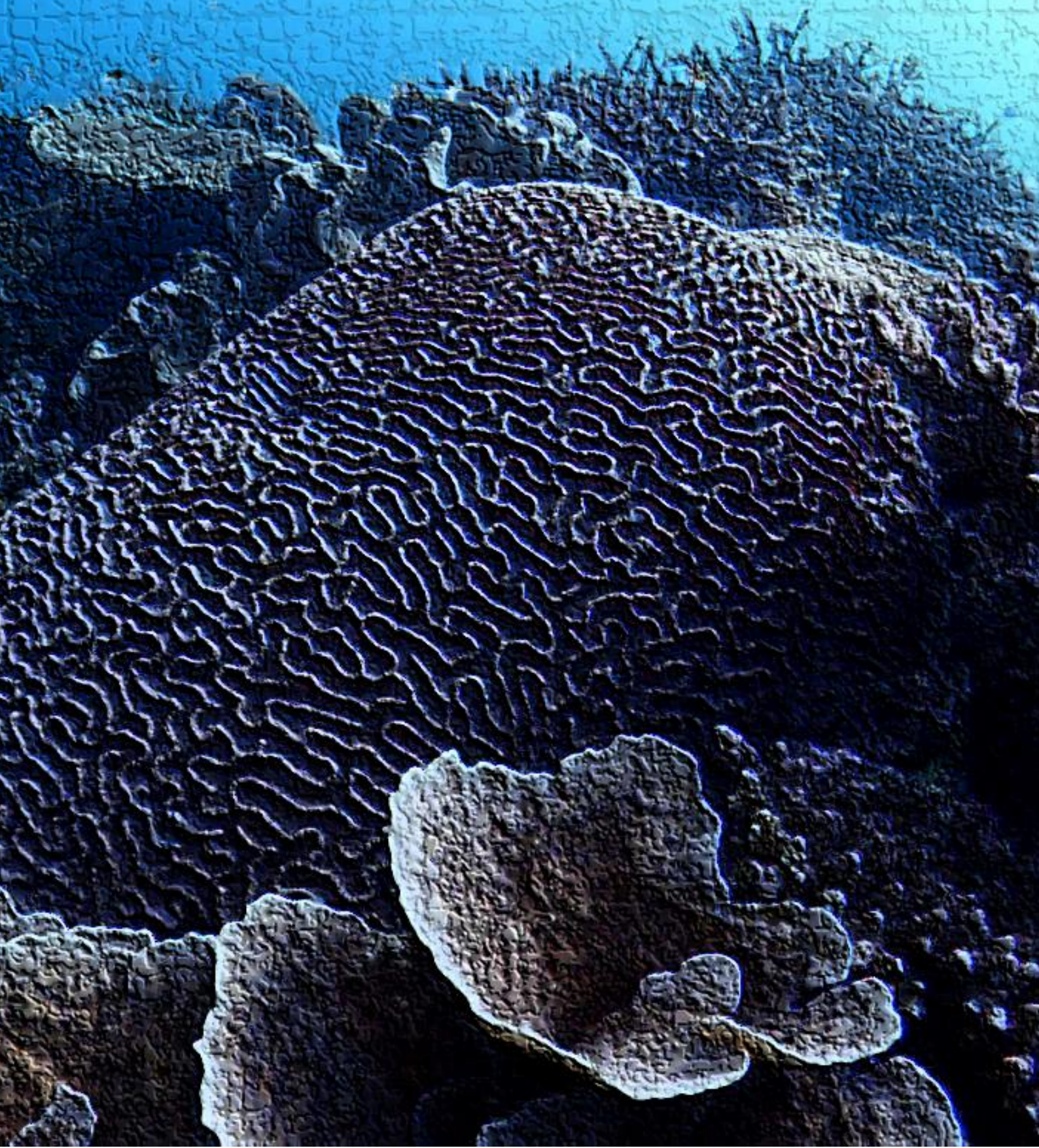


# Stability of artificial coral reefs in stormy weather conditions

SYTZE VEENLAND

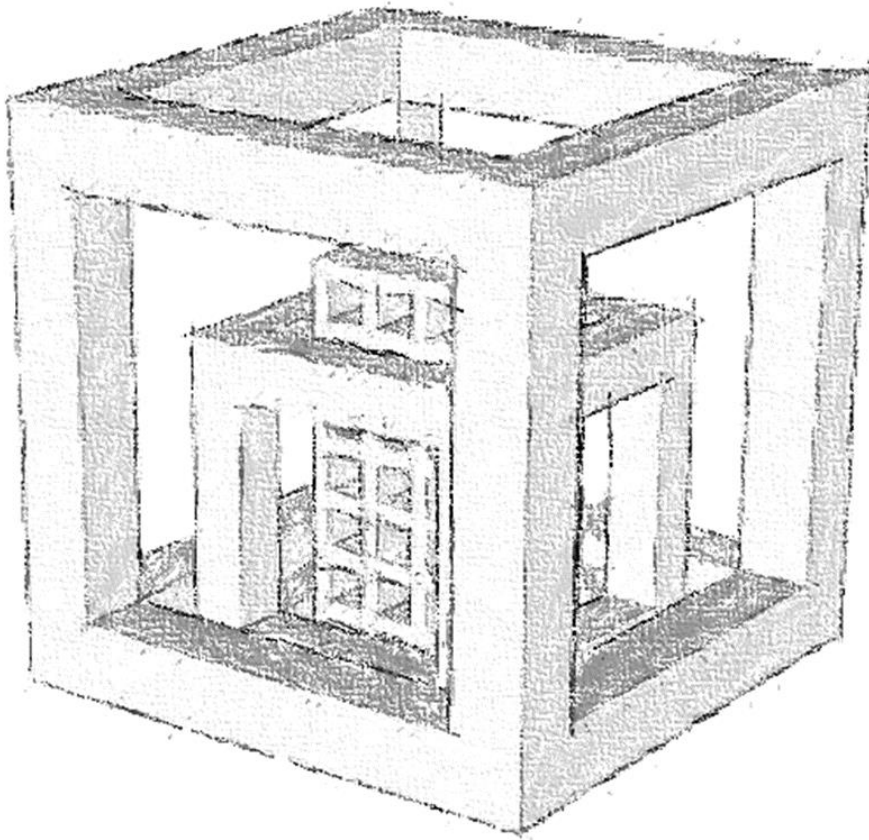


# Stability of artificial coral reefs in stormy weather conditions

A study on the stability of different configurations of concrete cube framework artificial coral reefs located at the north east coast of Bali, Indonesia.

by

Sytze Veenland



Student number: 5096626

Thesis supervisor: Dr. Ir. B. Hofland (Bas)

Second supervisor: Ir. D. C. P. van Kester (Dennis)

## Preface

This Bachelor thesis is carried out to complete my bachelor Civil Engineering at the TU Delft. I enjoyed spending my time on this project and this first encounter with writing a research report. This thesis is not just the finalization of my Bachelor degree, but is also an introduction to my next study journey: the master Civil Engineering at the TU Delft, where I will continue my learning path in the field of hydraulic engineering. During the creation of this thesis, I used the knowledge I obtained during my bachelor in Civil Engineering and obtained more knowledge about subjects related to hydraulic engineering. I want to thank dr. ir. B. Hofland and ir. D. C. P. van Kester for supervising my work and sharing their knowledge on the subject of Coastal Engineering. I also want to thank Rolf Voorhuis, CEO of Coral Reef Care, for supplying the needed information to complete this thesis.

Sytze Veenland,  
*Delft, June 2023*

## Abstract

Significant areas of coral reef are lost at the shoreline of Bali, Indonesia. Hard corals are demolished due to dynamite fishing. Coral Reef Care has installed artificial reefs to recreate the stable hard corals to restore the reef ecosystems. These structures became unstable during a storm in January 2023. In this thesis a study on the stability of these reef structures is executed to select a stable reef configuration which maintains a stable base for corals.

The location of the evaluated reefs is placed on the northeast shore of Bali. Firstly the offshore hydraulic design conditions are obtained, consisting of the significant wave height, wave period, bathymetry and water levels. These conditions are used as input for a SWAN 1D model, resulting in the nearshore hydraulic conditions. The nearshore conditions are used to calculate the orbital velocity at the depth of the reefs. The reefs are examined to obtain the physical parameters needed to quantify the present forces. These parameters are the volume, projected area of object normal to the flow direction, moment arms and the bottom friction-, drag- and lift coefficients. The forces on the reefs consist of the gravitational force, lift force, bottom friction force and drag force. A simple 2D horizontal force- and moment equilibrium model is made, using the determined forces. The model is calibrated by using the nearshore hydraulic conditions of two different storms, one of these storms (January 2023) resulted in instabilities of the structures. A structure design life time of 10 years is chosen and the structures are designed to resist a storm with a 50 year return period. This is done by using the nearshore data of this design storm as input for the equilibrium model.

The final configuration consists of a configuration of 2 columns and 6 rows of Cube L with Cube S and Bricks. Pipes are hammered in the ground and connected to the reef to secure the stability in case of the loss of bottom friction.

The low amount of data points of the bathymetry and the scarce availability of the water level data caused uncertainties in the SWAN model results and for the hydraulic conditions. The literature-based estimation of the physical parameters of the structure results in uncertainties in the stability model. The uncertainties of the hydraulic conditions can be limited by mapping the bottom profile more accurate and to measure the water levels at the location of the reefs with water pressure sensors. Wave flume research is recommended to increase the accuracy of the physical parameters of the structures.

# Table of contents

Preface.....	i
Abstract .....	ii
1. Introduction.....	1
1.1 Background information.....	1
1.2 Problem analysis.....	1
1.3 Objective.....	1
1.4 Approach .....	2
1.5 Scope .....	2
1.6 Reading guide .....	2
2. Site information and literature.....	3
2.1 Location .....	3
2.2 Configuration.....	3
3. Methodology .....	5
3.1 Offshore hydraulic storm conditions.....	5
3.2 Nearshore transformation .....	6
3.3 Forces on reef structure .....	7
3.4 Stability of the possible design configurations.....	9
4. Results .....	11
4.1 Offshore hydraulic storm conditions.....	11
4.2 Nearshore transformation .....	13
4.3 Forces on reef structure .....	13
4.4 Stability of the possible design configurations.....	14
5. Discussion .....	18
5.1 Evaluation of methodology .....	18
5.2 Evaluation of results .....	18
6. Conclusion: final configuration selection .....	19
7. Recommendations.....	20
Appendix A: Calculation of area normal projected to flow.....	21
Appendix B: Sonar map of Navionics (Navionics, 2023).....	25
Appendix C: SWAN 1D model.....	27
Appendix D: Python code for stability model.....	28
Literature.....	29

# 1. Introduction

## 1.1 Background information

Stable coral ecosystems are important to maintain biodiversity, for local fishers to be able to have enough fish in the future and for the tourism sector to attract tourists. Coral reefs are however degrading on various locations like Bali (Tito & Ampou, 2019). Coral reefs have been destroyed by blast fishing on Bali, among other locations (Hampton-Smith et al., 2021). The damage done by blast fishing can be repaired by constructing artificial coral reef structures. The coral can't regrow without a stable structure. Artificial reefs act as a stable base for the coral to grow on and as a hide-out for coral life. Coral Reef Care (CRC), a Dutch NGO, is designing and placing artificial coral reefs. Concrete- and steel structures are used as a new base for corals in their projects.

## 1.2 Problem analysis

The current reef configurations of CRC at the two most eastern reef locations (Lipah and Jemeluk) started to slide over the seafloor and various structures tilted more than 360 degrees due to a storm which took place in January 2023 as seen in Figure 1-1. CRC has added small cube frameworks and bricks with holes to their large cube framework structures to increase the possibilities for coral life of finding hide-outs in the artificial reefs. These additions could have caused an increase of drag forces on the structures.



Figure 1-1: Displacement of artificial coral reefs in January 2023 (Pictures from CRC).

The problem statement is formulated as follows:

*Artificial coral reefs used by Coral Reef Care should act as a stable base for corals, but under stormy weather conditions they become unstable and started to slide over the ocean floor.*

## 1.3 Objective

The thesis objective is formulated as follows:

*Evaluate and optimize a simple configuration of cube framework artificial reef structures, for reefs located at the north east shore of Bali, Indonesia, which remains stable during storm conditions.*

The sub questions are formulated as follows:

- What are the hydraulic design storm conditions at the north east coast of Bali, Indonesia?
- What combination of artificial reef structures result in a stable configuration during the design storm conditions?

## 1.4 Approach

To determine the stability of the artificial reefs, the governing offshore hydraulic storm conditions are needed. The important hydraulic conditions are the local bathymetry, the water levels and the offshore wave parameters. The bathymetry is retrieved from GEBCO (General Bathymetric Chart of the Oceans). The offshore wave parameters ( $H_s$ ,  $H_{dir}$ ,  $T_p$ ,  $v_{10}$ ,  $u_{10}$ ) are obtained through extreme value analysis of ECMWF ERA5-data over the time period from 1971 till 2022. The water levels are dominated by tide levels. The lower water levels cause a higher orbital velocity and are therefore governing. The offshore conditions influence the nearshore conditions by propagating towards the coast. The transformation from offshore to nearshore waves is determined with a SWAN 1D (Simulating WAVes Nearshore) wave model. Eventually the hydraulic conditions at the location of the reefs is determined, using linear wave theory. These nearshore hydraulic conditions consist of the orbital velocity and local depths. The magnitude of forces working on the reefs is determined via a simple 2D force model, calculating the force equilibria and moment equilibrium. The model is calibrated by using wave data since the installation of the reefs in November 2021. The stable configurations can be determined by changing the parameters used in the stability calculations ( $S$  (area normally projected to flow) and  $V$  (volume of structure according to different reef configurations)). The propagation of waves from offshore to the location is shown in Figure 1-2.

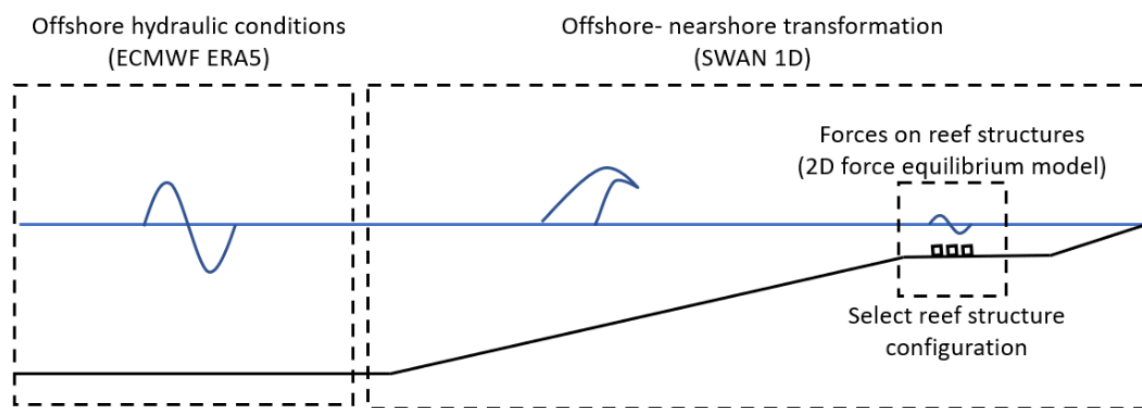


Figure 1-2: Propagation of waves from offshore to the project location.

## 1.5 Scope

The main focus is on the evaluation and optimization of the artificial reefs consisting of large cube frameworks, small cube frameworks and bricks with holes. Other structure designs are not in the scope of this report. The reef configurations will be assessed on the effect of the amount of large cubes used in a matrix formation and the presence of the small cubes and bricks. Also steel pipes are currently used to stabilize the structures, the force on the pipes will be chosen to be equal to the total drag force on the structures, this situation occurs when the whole structure loses contact with the bottom and the bottom friction forces become zero.

This thesis will focus on a single location at the north east shore of Bali, since this is the location (at Lipah and Jemeluk) where the artificial reefs started sliding during a storm in January 2023. The breaking of waves is assumed to not take place at the location of the artificial reefs.

## 1.6 Reading guide

Chapter 1 gives an introduction to the thesis. This introduction consist of the background information, problem analysis, objective, approach, scope and reading guide. Chapter 2 gives more specific information about the location and the current reef configuration. Chapter 3 explains the methodology of the research project. In chapter 4 the results of the steps are shown. In chapter 5 the results are discussed and possible errors are addressed. A final configuration of the artificial reefs is chosen in chapter 6. In chapter 7 the recommendations are given to Coral Reef Care and to future researchers on this subject.

## 2. Site information and literature

### 2.1 Location

CRC has placed artificial reefs on four different locations in Indonesia as shown in Figure 2-1. The location of the evaluated reef is located at -8,34 latitude 115,67 longitude, between Jemeluk and Lipah on the northeastern coast of Bali, Indonesia. These are the two locations where artificial reefs from CRC have been displaced and tilted. Few data sources are available at this location, reanalyzed ERA5 data is used to obtain the boundary conditions at the evaluated location. No instabilities occurred on the two western locations. This is most probably caused by the bigger depth on which these reefs are placed, resulting in lower orbital velocities. The depth of the two western locations is approximately 10 meters, while the eastern reefs are at 3 to 5 meters depth. The reefs are placed at a distance of 100 meters from the shoreline.



Figure 2-1: Highlighted artificial coral reef locations of CRC on Bali, Indonesia (Google, 2023).

The bottom of the assessed location is covered with old coral rubble and sand. There are no signs of scour at the location of the reefs, so this has caused no instabilities for the structures and will not be taken into account.

### 2.2 Configuration

There are three different structures used for the artificial reefs of CRC. These structures are the Cube L, Cube S and Brick as seen in Figure 2-2. All structures are made of concrete and by local labor. The Cube L structures are connected to each other with rope to create a bigger artificial reef and to make a more stable structure. The Cube S and the Bricks are added to the structure to give small coral life the possibility to hide from predators, as seen in Figure 2-3 (Diringer, 2021). The configuration used when the reefs became unstable consisted of 4 Cube L's tied together, with 1 Cube S and 2 Bricks inside each Cube L. The configuration used after the instability occurred consists of 2 columns of 7 Cube L's without Bricks and only 30% of the Cube L's contain a Cube S. A structure life time of approximate 10 years is needed to grow the corals to a more resilient ecosystem.

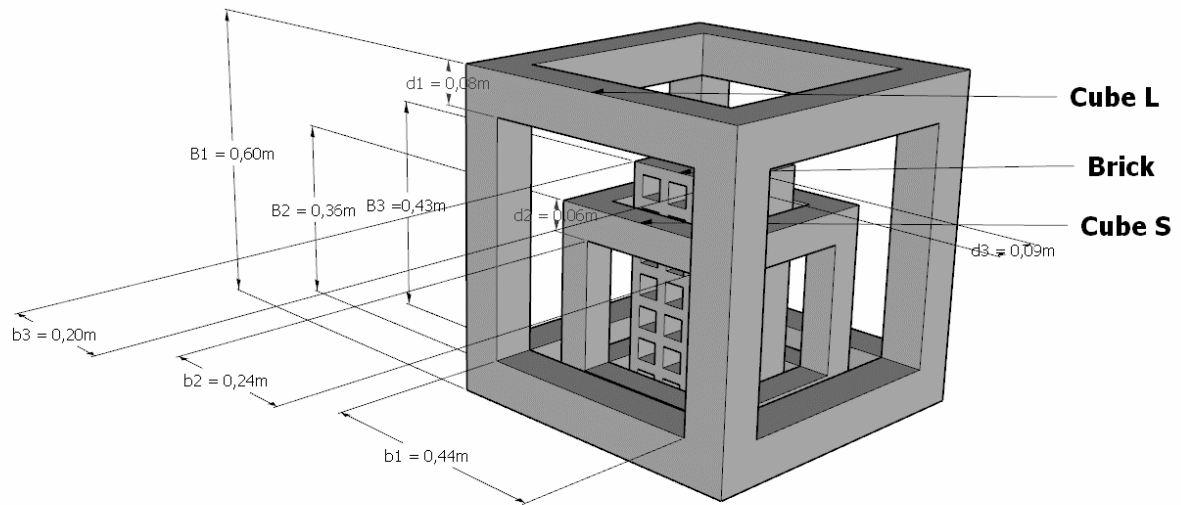


Figure 2-2: Cube L, Cube S and the Brick, used by Coral Reef Care.

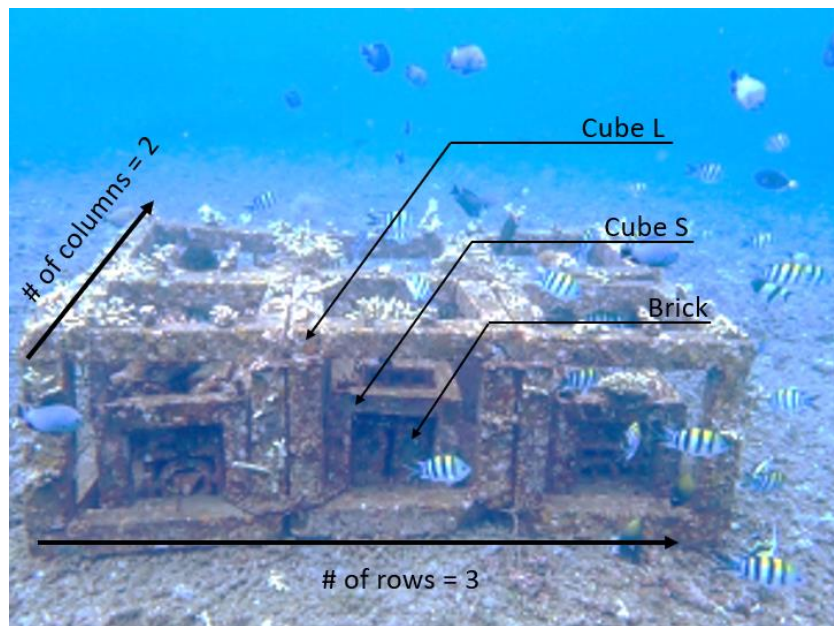


Figure 2-3: A reef configuration of CRC with 6 Cube L's (Picture from CRC).

The design conditions are chosen to have a return time of 50 years to ensure a safe reef configuration. These design conditions have a probability of exceedance of 18.3% for a life time of 10 years, according to the following formula (Jonkman et al., 2017):

$$R = 1 - \left(1 - \left(\frac{1}{T}\right)^n\right)$$

In which:

$n$ : design life time of structure [years]

$T$ : mean return time of storm [years]

$R$ : probability of exceedance of storm conditions with return time  $T$  [-]

### 3 Methodology

This chapter deals with the methodology used for the evaluation and optimization of the stability of artificial coral reefs. This chapter is split into four sections. At first the methodology to obtain the design offshore hydraulic storm conditions is explained. Secondly the SWAN 1D setup to determine the nearshore transformation is dealt with. Thirdly the forces, caused by the hydraulic conditions and acting on the reef structures, are examined. At last the force- and moment equilibria of the structures are prescribed.

#### 3.1 Offshore hydraulic storm conditions

The offshore hydraulic storm conditions influence the stability of the reef structures. The design conditions are chosen to have a return time of 50 years to ensure a save reef configuration. The offshore wave data from the storm which caused the instabilities in the beginning of 2023 is available from ERA5 (Hersbach et al., 2023). Therefore the eventual stability model can be calibrated in respect of that storm event.

##### **Bathymetry**

The local bathymetry data is obtained from GEBCO for the region -6 to -9 degrees latitude and 114 to 117 degrees longitude (GEBCO, 2023). This data is downloaded in a netCDF-file and plotted in the Python environment Jupiter Lab using Matplotlib Basemap. The 2D bathymetry profile to be used in SWAN is chosen to be perpendicular to the depth lines along the shore.

##### **Offshore wave conditions**

The data for offshore waves is retrieved from ERA5 ECMWF. The data over the period 1971-2022 at a 2-hours interval is obtained from the location at -8.2 latitude and 115.7 longitude. This location, as well as the location of the artificial reefs, is plotted in Figure 3-1. The variables selected from the ERA5 data are the significant height of combined wind waves and swell ( $H_s$ ), the mean wave period ( $T_p$ ), the mean wave direction ( $H_{dir}$ ) and the 10m u- and v- components of the wind at 10 meters above sea level ( $u_{10}$ ,  $v_{10}$ ).

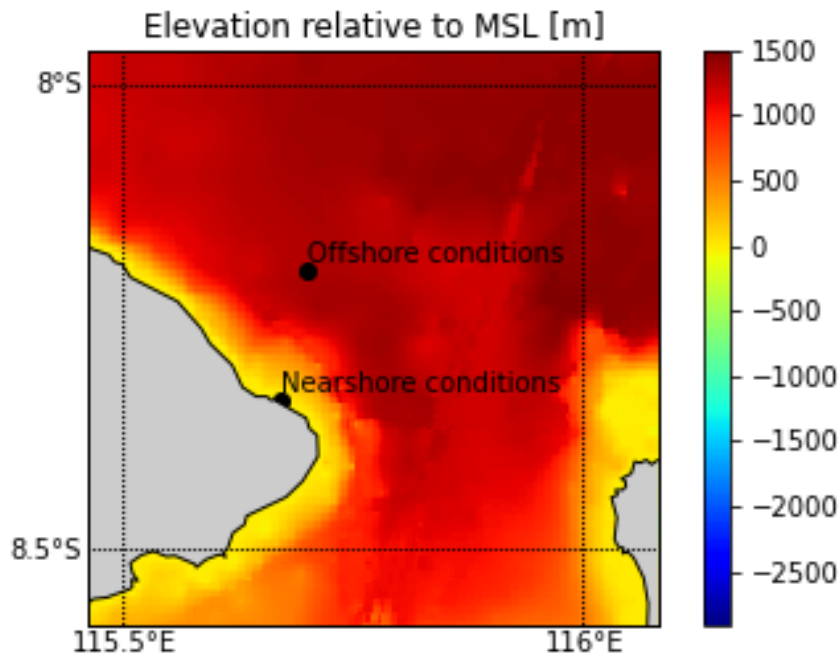


Figure 3-1: Location of offshore datapoint and location of the to be examined reef.

The obtained data of the significant wave heights is examined using extreme value analysis. From the ERA5 data from 1971-2022, with intervals of 2 hours, the highest significant wave height is selected for each year. This results in a dataset of significant wave heights and their return periods.

### Extreme water levels

The final offshore hydraulic condition is the water level. The total water level is the combination of tide levels and wind set-up levels. The lowest water level results in the highest orbital velocities. Wind set-up is not taken into account, since this only results in higher water levels, causing lower orbital velocities. Tide data is found via online tide charts from tidechart.com (tidechart.com, 2023). The governing tide level is the LAT (lowest astronomical tide), since a lower water level results in higher orbital velocities at the ocean bottom.

### 3.2 Nearshore transformation

SWAN 1D is used for the transformation of waves from the offshore to nearshore state. The model setup is described in this section. The model input consists of the bathymetry, grid, boundary conditions, physical parameters and the output lines.

#### Bathymetry

The bathymetry is obtained from GEBCO in section 4.1 and is loaded in SWAN. The bathymetry is one dimensional and chosen to be perpendicular to the depth lines.

#### Grid

A 1D grid is used with spherical coordinates. The origin of the grid is in point (-8.34; 115.67) and is directed in an angle of 11.7 degrees from the north as seen in Figure 3-2.

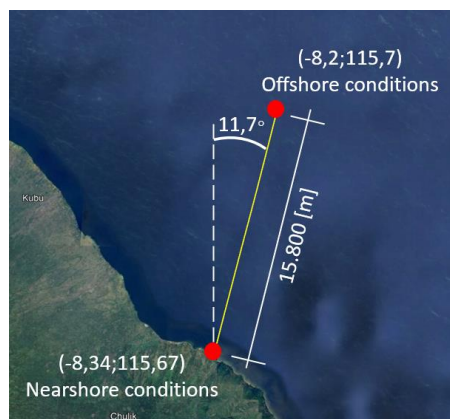


Figure 3-2: Grid coordinates used in SWAN (Google, 2023).

#### Boundary conditions

The boundary condition is applied as an JONSWAP spectrum on the north side of the grid, at the offshore side. The boundary conditions consist of the wave height and period. These conditions are obtained in section 4.1. The wave direction is obtained by the ERA5 data.

#### Physical parameters

Breaking, refraction, friction and wind velocity are used as input for the physical parameters. Refraction is an important physical parameter, since the wave direction is not perpendicular to the shore.

#### Output

A table with the coordinates, significant wave heights, wave period, wave direction, water depth and the wave length is retrieved from the SWAN model. The relevant nearshore hydraulic conditions are obtained from this table.

#### Design wave height

Not the significant wave height, but the design wave height is used to determine the forces acting on the reef structures, since the stability during storm conditions is examined. A Rayleigh distribution of the waves is assumed. The nearshore significant wave height follows from the SWAN model. As the design wave height, the 1% highest waves are selected:  $\Pr(H > H_d) = 0.01$ .

The design wave height is calculated with the following formula, assuming a Rayleigh distribution for the wave height spectrum (Longuet-Higgins, 1952):

$$H_d = \sqrt{-\frac{1}{2} \ln \left( \frac{-\ln(1 - \text{Pr}(H > H_d))}{N} \right)} \cdot H_s \text{ [m]} \quad (1)$$

In which:

$$N = \frac{T_{storm}}{T_{wave}} \text{ [-]}$$

$H_d$ : design wave height [m]

$\text{Pr}(H > H_d)$ : probability of waves being higher than the design wave height [-]

$T_{storm}$ : storm period [s]

$T_{wave}$ : wave period [s]

$H_s$ : significant wave height [m]

This formula may not be totally accurate due to the shallow water at the location of the artificial reefs. The formula will give conservative results, so could still be used. Wave heights are limited by the water depth with the following equation (Massel, 1996):  $\frac{\text{wave height}}{\text{water depth}} = 0.6 \text{ [-]}$ .

### 3.3 Forces on reef structure

The design wave height and wave periods obtained by SWAN are used to determine the forces on the structures. First the orbital velocity is determined. The orbital velocity influences the magnitude of the forces on the structure. The orbital velocity is schematized in Figure 3-3.

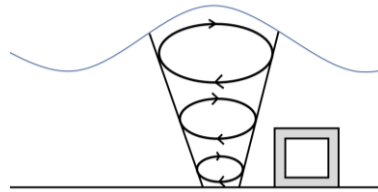


Figure 3-3: Orbital velocity underneath a wave.

The determination of vertical and horizontal orbital velocity is done with respectively the following formulas (Kamphuis, 2000):

$$u = \frac{\pi H}{T} \cdot \frac{\cosh(k(z+d))}{\sinh(kd)} \cos(kx - \omega t) \left[ \frac{m}{s} \right] \quad (2)$$

$$w = \frac{\pi H}{T} \cdot \frac{\sinh k(z+d)}{\sinh(kd)} \sin(kx - \omega t) \left[ \frac{m}{s} \right] \quad (3)$$

In which:

$H$ : wave height [m]

$T$ : wave period [s]

$k$ : wave number  $\left( \frac{2\pi}{L} \right) \text{ [m}^{-1}\text{]}$

$L$ : wave length [m]

$c$ : wave celerity [m/s]

$z$ : upward vertical distance above still water [m]

$d$ : depth of water [m]

$x$ : horizontal direction [m]

$\omega$ : wave angular velocity  $\left( \frac{2\pi}{T} \right) \left[ \frac{rad}{s} \right]$

$t$ : time [s]

The parameters used in the orbital velocity equation are obtained via the SWAN model results. The values of the horizontal direction and time can be set at 0, resulting in the loss of the  $\cos(kx - \omega t)$  term.  $-z$  is equal to  $d$ , for the location at the sea bottom. The vertical velocity will be negligible at the bottom of the ocean, since  $\sinh(k(z + d))$  is equal to zero when  $-z$  is equal to  $d$ . The final equation is as follows:

$$u = \frac{\pi H}{T \cdot \sinh(kd)} \left[ \frac{m}{s} \right] \quad (4)$$

The difference of the orbital velocity over the height of the reef structures is in the order of 0.1% and is therefore neglectable.

To determine the forces on the structures, different parameters and coefficients of the structures are needed. The bottom friction coefficient is chosen to be 0.6 (Siderius, 2022). A sensitivity analysis for the bottom friction coefficient is executed in section 4.4, since the bottom friction coefficient could vary due to the presence of loose coral rubble with algae.

The forces are working on the three different structures, the Cube L, Cube S and the Bricks. Different parameters of these structures are shown in Table 3-1. The parameter V (volume of structure) is calculated by using the known structure dimensions. The parameter S (projected area normal to the flow) is split in 6 different values for different cube configurations. A different value for S is obtained for the empty Cube L ( $S_1$ ), the Cube L with Cube S ( $S_2$ ) and the Cube L with Cube S and Bricks ( $S_3$ ). The area S of the front row of cubes is also different than the area S of the cubes behind the first row ( $S_4, S_5$  and  $S_6$ ). This is because the first row of cubes obstruct the water flowing towards the rows in behind. The calculation of the values of  $S_1, S_2, S_3, S_4, S_5$  and  $S_6$  are shown in Appendix A; the results are displayed in Table 3-2. For the specific weight of the concrete a value of  $2100 \text{ kg/m}^3$  is measured for the Cubes and a value of  $1900 \text{ kg/m}^3$  for the Bricks. This difference is caused by the presence of steel reinforcement bars in the Cubes. The value of  $C_D$  depends on the Reynolds number (Reynolds, 1883):

$$Re = \frac{\rho_w u D}{\mu} [-] \quad (5)$$

In which:

$$\begin{aligned} Re: & \text{Reynolds number } [-] \\ \rho_w: & \text{specific weight of water } [\text{kg/m}^3] \\ u: & \text{velocity of fluid } \left[ \frac{m}{s} \right] \\ D: & \text{characteristic dimension (width of rod)} [m] \\ \mu_{viscosity}: & \text{dynamic viscosity of the fluid } [\text{Pa} \cdot \text{s}] \end{aligned}$$

In case of the cube frameworks with a dimension of 0.6 [m] and an orbital velocity of 2 [m/s], the following Reynolds number is obtained from formula 5:

$$Re = \frac{1025 \cdot 2.0 \cdot 0.6}{1.0016 \cdot 10^{-3}} = 1.63 \cdot 10^5 [-]$$

A  $C_D$  of 1.2 [-] is used for rounded rods for this value of the Reynolds number, this is selected to be the lower bound of the used  $C_D$  values (Wieselsberger & United, 1922). For 3D squares a  $C_D$  value of 1.05 is found and for a square rod, placed between walls, a  $C_D$  of 2.05 [-] is found (Hoerner, 1965). A range from 1.2 to 1.8 [-] is selected for the possible  $C_D$  values.

	V [m <sup>3</sup> ]	$\rho_s$ [kg/m <sup>3</sup> ]	$C_D$ [-]	$C_L$ [-]
<b>Cube L</b>	0.037888	2100	1.2-1.8	0.2
<b>Cube S</b>	0.012096	2100	1.2-1.8	0.2
<b>Brick</b>	0.005425	1900	1.2-1.8	0.2

Table 3-1: Parameters of different artificial reef structures.

Configuration	$S [m^2]$
$S_1$	0.3072
$S_2$	0.3776
$S_3$	0.4068
$S_4$	0.1408
$S_5$	0.2112
$S_6$	0.2404

Table 3-2: Area normal to flow for different Cube configurations.

The artificial reefs are subjected by 5 forces, namely the drag force ( $F_D$ ), gravitational force ( $F_G$ ), bottom friction force ( $F_B$ ), lift force ( $F_L$ ) and the inertia force ( $F_I$ ). Since the cube frameworks are slender ( $\frac{L}{D} = \frac{40}{0.6} \ll 5$ ), the inertia force is neglected for the stability calculations. The present forces are calculated with formula 6, 7, 8 and 9 (Elger et al., 2020):

$$F_D = \frac{1}{2} C_D \rho_w S u^2 \quad (6)$$

$$F_G = (\rho_s - \rho_w) g V \quad (7)$$

$$F_B = \mu (F_G - F_L) \quad (8)$$

$$F_L = \frac{1}{2} C_L \rho_w S u^2 \quad (9)$$

In which:

$\rho_w$ : specific weight of water [ $kg/m^3$ ]

$\rho_s$ : specific weight of object [ $kg/m^3$ ]

$g$ : gravitational acceleration [ $m/s^2$ ]

$u$ : velocity of object relative to the fluid [ $m/s$ ]

$S$ : projected area of object normal to the force direction [ $m^2$ ]

$V$ : volume of object [ $m^3$ ]

$\mu$ : bottom friction coefficient [-]

$C_D$ : drag coefficient [-]

$C_L$ : lift coefficient [-]

### 3.4 Stability of the possible design configurations

When the forces on the structure are quantified, stability of the artificial reefs has to be determined by the force- and moment equilibria. Figure 3-4 shows the forces acting on the artificial reefs.

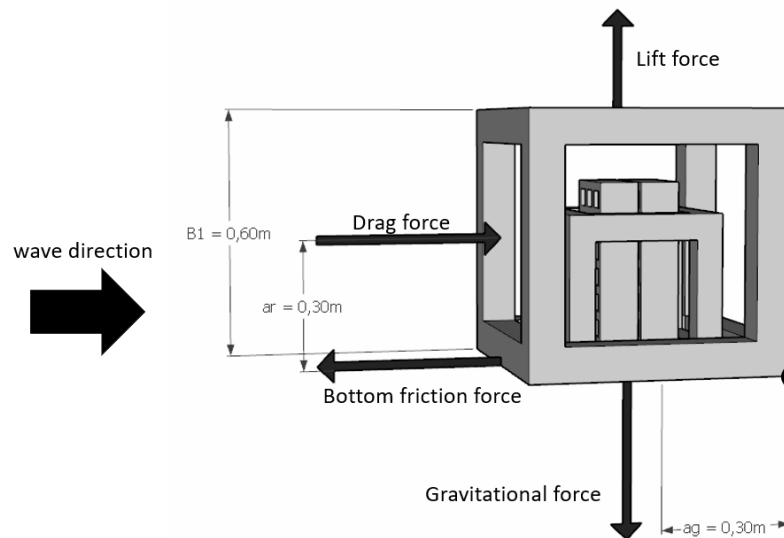


Figure 3-4: Forces acting on the artificial reefs

To determine the force equilibria the following equilibria are used:

$$\sum F_h = 0; \sum M = 0 \quad (\mathbf{10}; \mathbf{11}).$$

A vertical moment arm  $a_r = 0.3$  [m] is selected for the drag forces for each configuration. This is conservative for the Cube L with Cube S and Bricks, since the center of the area is lower, caused by the addition of the Cube S and the Bricks. The horizontal moment arm ( $a_g$ ), used for resulting moments of the lift and gravitational force, is the amount of rows multiplied with  $\frac{1}{2} \cdot B_1$ , in which  $B_1$  is the length of Cube L, which is equal to 0.6 [m].

## 4 Results

In this chapter the results are shown following from the applied methodology of chapter 3.

### 4.1 Offshore hydraulic storm conditions

#### Bathymetry

The local bathymetry retrieved from GEBCO is shown in Figure 4-1. The data points are quadratically interpolated to obtain the full bathymetry. The density of data points is low. A slightly different bathymetry changes the wave transformation significantly, especially close to the shore. The gradual increase in depth however seems to correspond to the sonar chart of Navionics as seen in Figure 4-2 (Navionics, 2023). A more detailed sonar map is included in Appendix B.

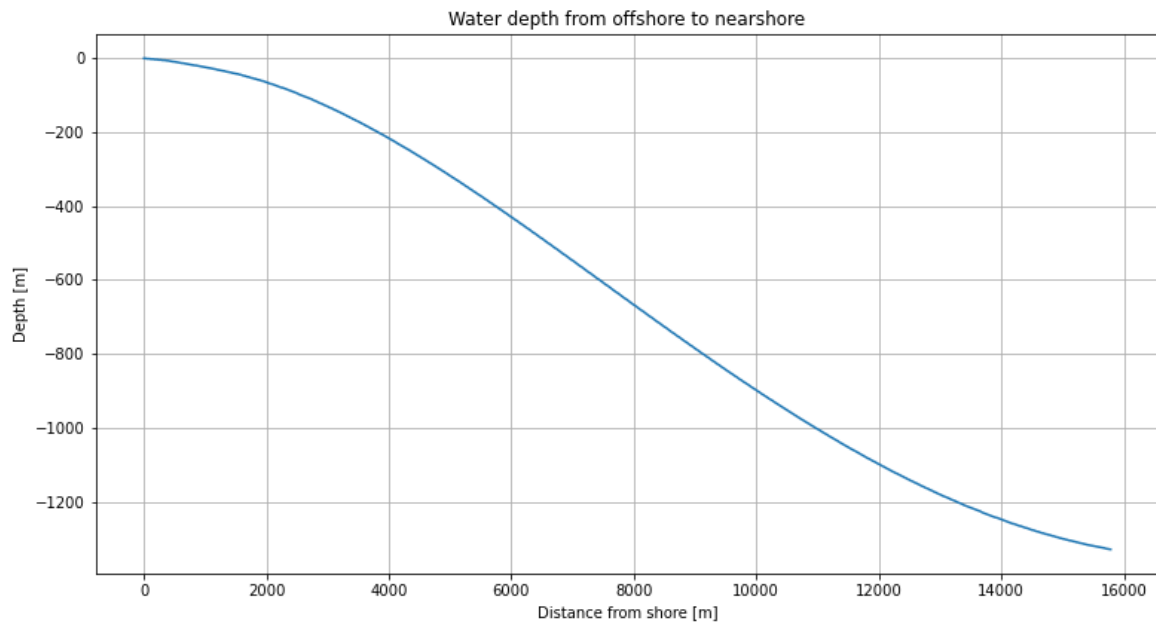


Figure 4-1: Simplified bathymetry of the Bali shore.



Figure 4-2: Sonar chart of Bali (Navionics, 2023).

### Offshore wave conditions

All offshore wave data is extracted from ERA5 ECMWF at the location of -8.2 latitude and 115.7 longitude. A scatter plot of all wave heights and their wave direction is shown in Figure 4-3. Only the maximum significant wave height per year is taken into account for the extreme value analysis. These selected values are plotted with orange dots. A wave direction of 300 degrees is chosen to be used for the boundary conditions of the SWAN 1D model.

The selected values are plotted against their wave period in Figure 4-4. During the storm in the first days of January 2023, the mean wave period was 7 seconds. The maximum wave steepness  $s_{op}$  is 0.0335 [-]. This value is obtained by plotting  $s_{op} = \frac{H}{1.56 \cdot T_p^2}$  in Figure 4-4.

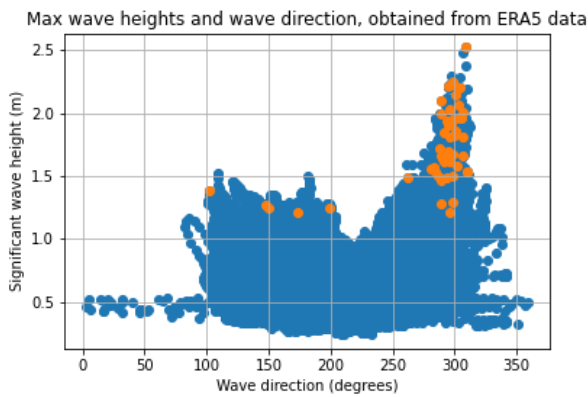


Figure 4-3: Significant wave heights and their governing wave direction.

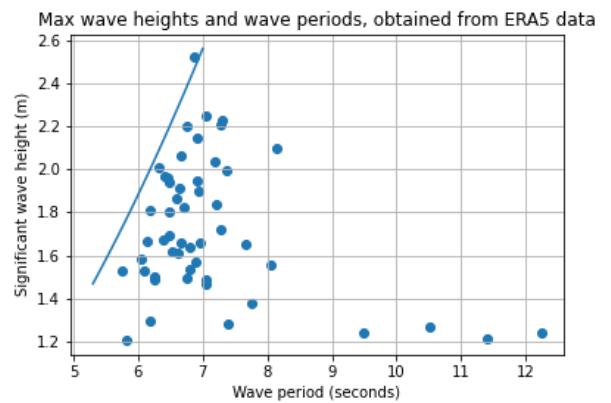


Figure 4-4: Maximum significant wave heights per year and their wave directions.

Now the return times are determined by plotting the sorted maximum wave heights. The return times for different significant wave heights are plotted in Figure 4-5. These points are linearly fitted. A logarithmic scale is normally used to extrapolate the return periods. In this case the data is not extrapolated, since the needed return periods are already known from the extracted data. For the structure a life time of 10 years is given. The design conditions are chosen to have a return period of 50 years. The significant wave height corresponding to a 50 year return period is 2.5 meters.

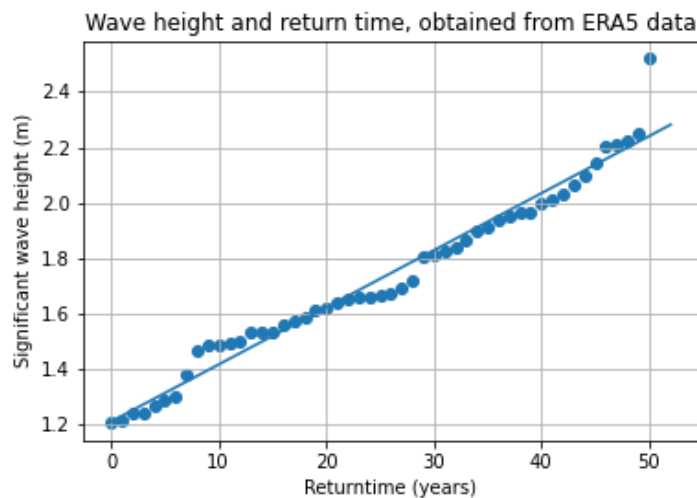


Figure 4-5: Significant wave height per return period.

The wave period is determined from Figure 4-4, the significant wave period of the highest significant wave height from the offshore conditions is 6.8 seconds.

## Water levels

The tide amplitude in Abang, the region of the selected reef location, is 0.5 [m]. The difference in low and high tide is 1 [m] (tidechart.com, 2023). A water level of MSL -0.5 [m] is selected for the governing offshore conditions. However a water level of MSL +0.5 [m] results in higher values of  $H_s$ , the orbital velocity at the depth of the reef will be lower due to the increased water depth.

## 4.2 Nearshore transformation

The model code for the wave transformation in SWAN 1D is stated in Appendix C.

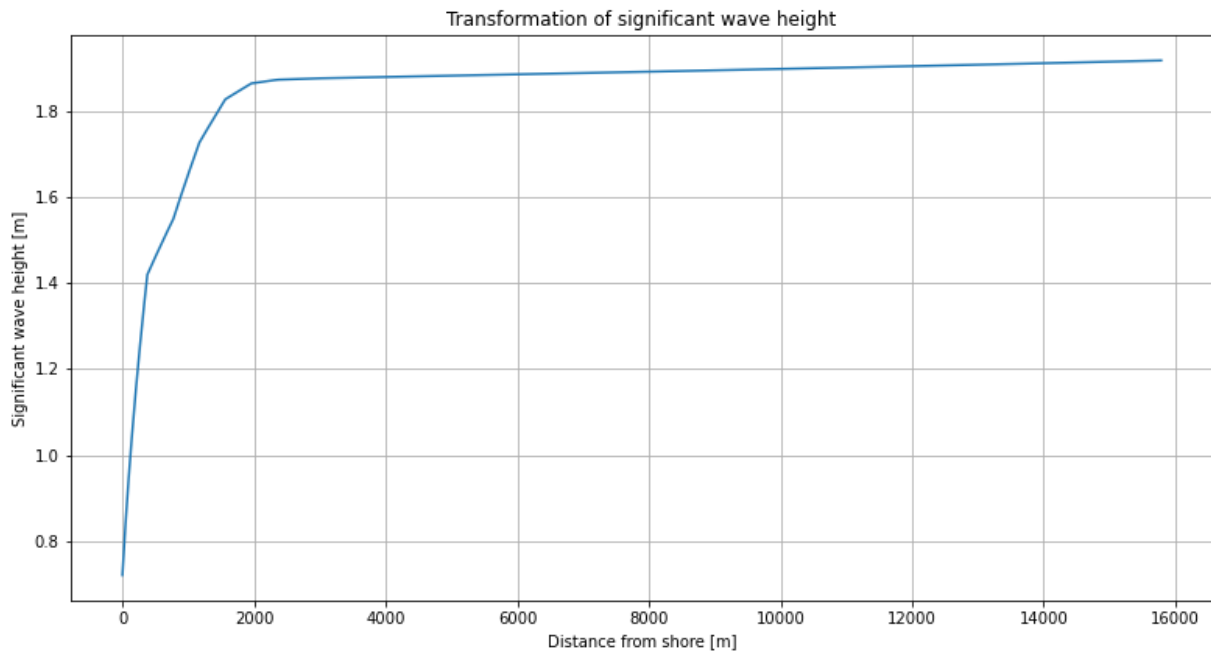


Figure 4-6: Transformation from offshore waves to nearshore waves.

The transformation of the significant wave height is shown in Figure 4-6. The SWAN model output at the location of the reefs, at 100m distance from the coastline, is shown in Table 4-1. These are the nearshore hydraulic conditions used as input for the stability model.

Parameter	Value
$H_s$	0.98 [m]
$T_p$	6.85 [s]
$L$	35.77 [m]
$d$	3.03 [m]

Table 4-1: Output of SWAN-model at 100 m from coastline for design conditions.

Formula 1 is used for the calculation of the peak wave height. This results in a design wave height  $H_d$  of 2.35 meters, using a storm period of 2 hours and a wave period of 6.85 seconds. This wave will not occur in waters with a depth of 3.03. The wave height will be limited to  $d \cdot 0.6 = 1.818$  [m].

## 4.3 Forces on reef structure

The orbital velocity at the bottom during the design conditions, corresponding to a return time of 50 years, is calculated with formula 4:

$$u \left[ \frac{m}{s} \right] = \frac{\pi H}{T \cdot \sinh(kd)} = \frac{\pi \cdot 1.818}{6.85 \cdot \sinh\left(\frac{2\pi}{35.77} \cdot 3.03\right)} = 1.495 \left[ \frac{m}{s} \right]$$

With formulas 6, 7, 8 and 9, from section 3.3, the forces on the different structures are determined.

#### 4.4 Stability of the possible design configurations

A Python model is created to compute the forces and the resulting force equilibria of the configurations. The model code is shown in Appendix D. The input of the model consists of:

- Significant wave height [m] (obtained by SWAN 1D)
- Wave period [s] (obtained by SWAN 1D)
- Depth [m] (obtained by SWAN 1D)
- Maximum wave length [m] (obtained by SWAN 1D)
- The amount of Cube L [# columns, # rows]
- The presence of Cube S [yes/no]
- The presence of Bricks [yes/no]

The model determines a design wave height by using formula 1. The design wave height is used with the nearshore conditions to determine the orbital velocity. The orbital velocity is used in combination with the physical parameters to determine the forces on the structure. A horizontal force equilibrium and a moment equilibrium is calculated with the model. The bottom friction force is larger than the drag force when the sum of horizontal forces is positive, resulting in a stable configuration.

The ERA5 data, during the period over which the reefs were active (11-2021 till 03-2023), is analyzed to calibrate the stability model. The reefs only became unstable during the storm in January 2023. The storm in January corresponds with the highest significant wave height since the installation of the reef, as seen in Figure 4-7. The standard reef configuration should remain stable during the hydraulic conditions of January 2022 but become unstable during the conditions of January 2023.

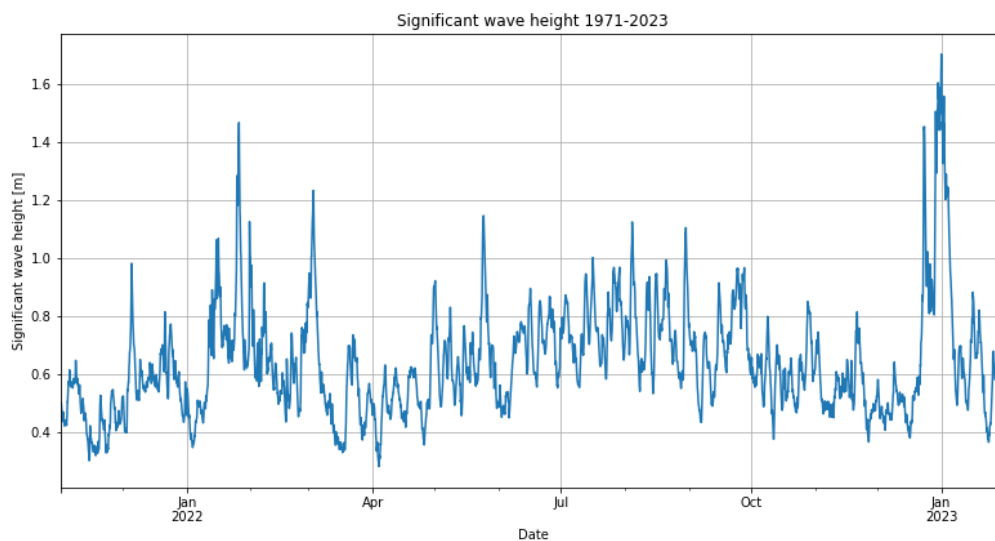


Figure 4-7: Offshore significant wave heights during the active period of reefs.

Also the wave period should be taken into account for the calibration of the model. The storm in 2023 corresponds with higher wave periods than the storm in 2022 as seen in Figure 4-8, resulting in higher orbital velocities.

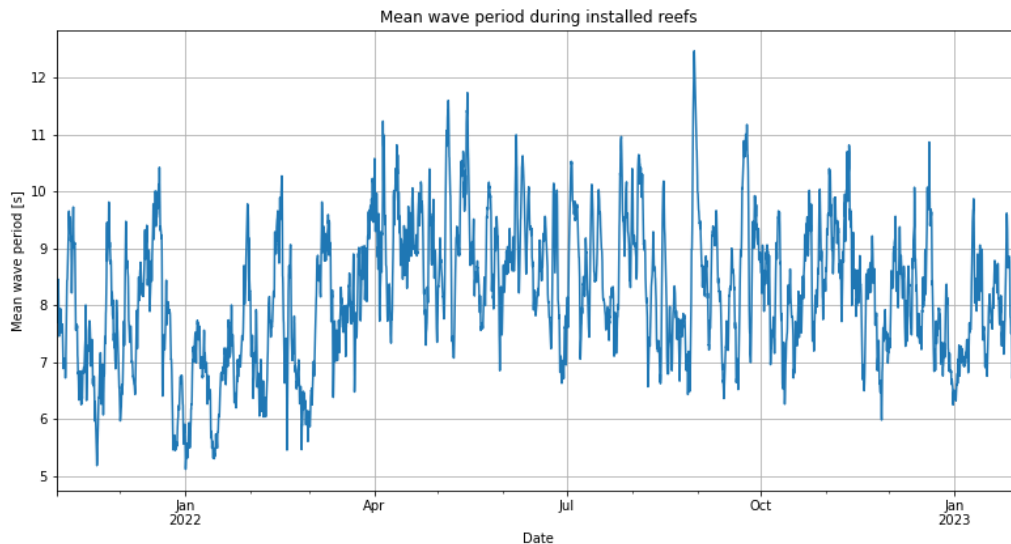


Figure 4-8: Offshore mean wave periods during the active period of reefs.

	January 2022 storm	January 2023 storm
$H_s$ [m]	0.66	0.75
$T_p$ [s]	5.96	7.18
$d$ [m]	3.03	3.03
$L_{max}$ [m]	30.66	35.77

Table 4-2: Results from SWAN 1D at 100 [m] from shore.

By using the nearshore hydraulic conditions of both storms as input for the model, the model can be calibrated and tested. These nearshore hydraulic conditions are shown in Table 4-2. The final model gives a stable situation for the 2022 storm and an unstable situation for the 2023 storm, using the configuration of the 2 by 2 Cube L and using the Cube S and the bricks. For these conditions a sensitivity analysis of the drag coefficient is executed. The result is plotted in Figure 4-9. The drag coefficient should be between 1.0 and 1.25 to give a stable situation in 2022 and a unstable situation in 2023. The positive forces are directed toward the offshore. A negative sum of forces results in an unstable configuration.

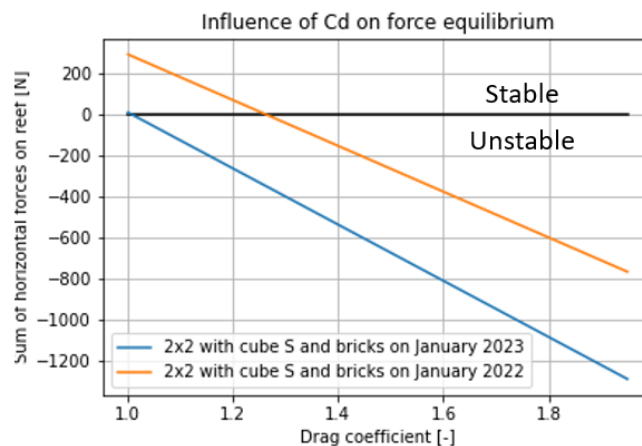


Figure 4-9: Sensitivity analysis of drag coefficient.

The model gives a stable situation for the 2023 storm if a configuration of 2 by 4 Cube L is used, including the Cube S and the Bricks. The presence of the Cube S and the Bricks seems to be a positive factor for the stability of the reefs. The added weight results in a higher bottom friction force. After the storm in 2023, the Bricks were scattered over the ocean bottom in some cases. This caused a loss of weight for the total configuration.

The conditions for which a stable configuration will be selected are the conditions with a 50 year return period. First the influence of the amount of rows is investigated, resulting in Figure 4-10. The configuration with both the Cube S and the Bricks is most stable and should be stable during design conditions when 6 or more rows are used. When this configuration loses the Bricks, it will however become unstable. A configuration of 6 rows is selected, since this configuration remains stable during design storm conditions. The Bricks should be attached firmly; if they leave the structure, the structure becomes unstable.

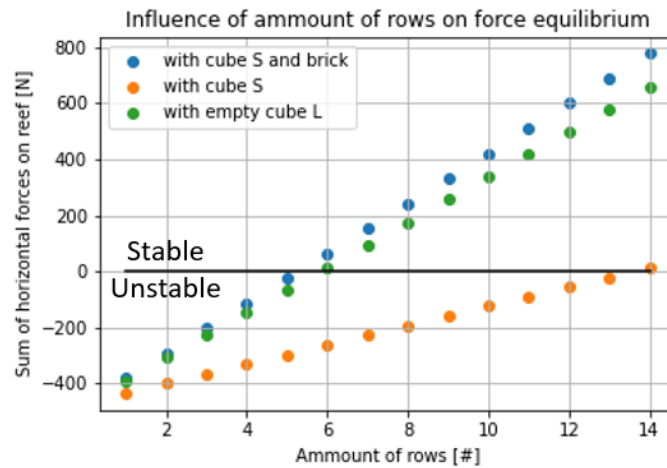


Figure 4-10: Stability of configurations with different number or rows.

Also a sensitivity analysis for the water depth is made. In this analysis the design hydraulic conditions are assumed to stay the same as in earlier calculations. Another depth will however change the nearshore wave transformation and will therefore result in different hydraulic conditions at the location of the reef. It is important to analyze the hydraulic conditions for new locations when a new reef is installed, the sensitivity analysis of the depth for the reefs in Bali cannot be applied for each location. The results on the sensitivity analysis of the depth is shown in Figure 4-11. The sudden jump in the graph at a depth of around 4 meters is caused by the restricted wave heights by the shallow water. The analysis of different depth shows that the empty Cube L is more stable in shallow water than the Cube L with Cube S. In deeper water the Cube L with Cube S becomes more stable.

A final sensitivity analysis is done for the bottom friction coefficient. The results are shown in Figure 4-12. The empty Cube L is the least sensitive for changes in the bottom friction coefficient. The bottom friction coefficient can possibly vary from the initial value, due to the presence of coral rubble and algae at the location of the reefs.

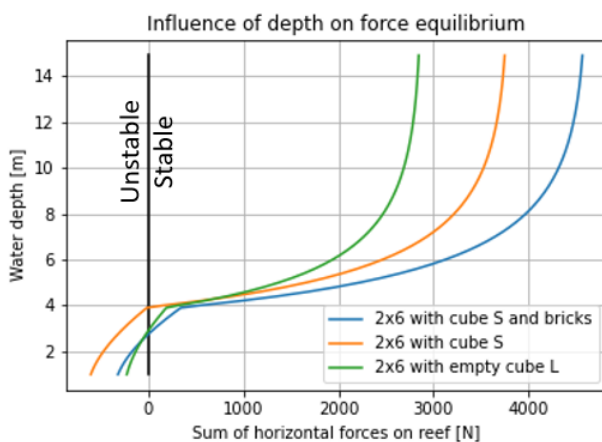


Figure 4-11: Sensitivity analysis of depth.

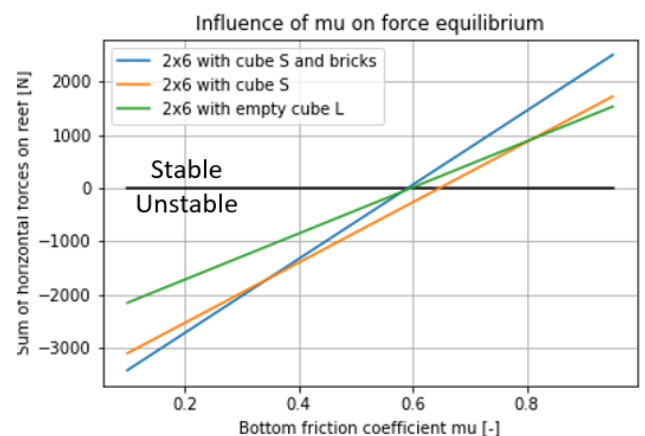


Figure 4-12: Sensitivity analysis of bottom friction coefficient.

Finally the total drag force on the structure is shown in Figure 4-13. This is the force working on the pipes, which are driven in the ground for stability purposes, when the structure would come loose from the bottom. The pipes should be able to bear a total horizontal force of 4100 Newton when a 6x2 configuration is selected with Cube S and Bricks.

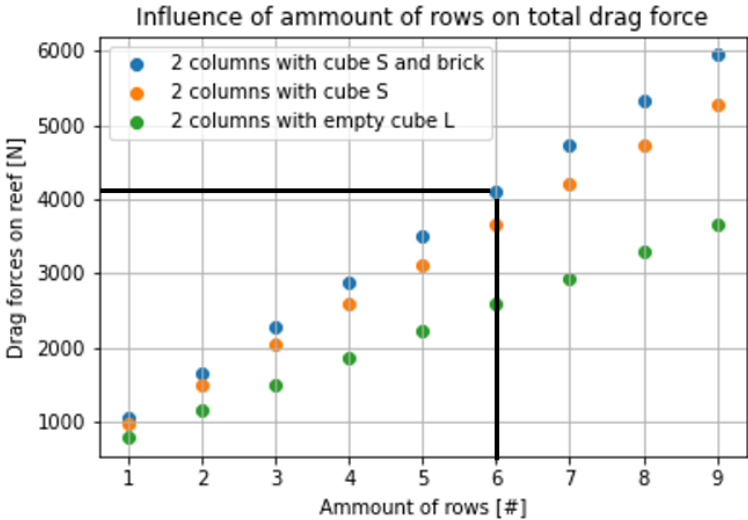


Figure 4-13: Total drag force on structure.

When the pipes are installed to secure the horizontal stability, the possibility of sliding is restricted. The moment equilibrium becomes more important in this situation. The pipes should be installed on the side of the reef at which the waves are coming in. This is shown in Figure 4-14. The reefs will start to tumble if the pipes are installed behind the structure.

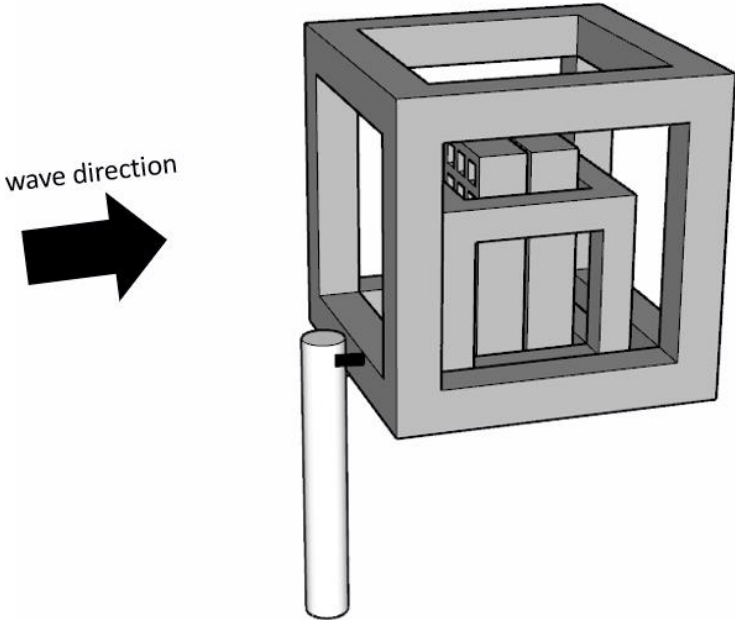


Figure 4-14: Advised placement of steel pipes.

## 5 Discussion

This chapter discusses the methodology and the results of this thesis.

### 5.1 Evaluation of methodology

#### **Offshore conditions**

Only few datapoints are found for the bathymetry, resulting in uncertainties in the bottom profile. This could influence the wave transformation significantly, causing different orbital velocities to be present at the location of the reefs. The water levels are determined using graphs from websites. These graphs showed the water levels for a period of only a week. This could result in the wrong water levels, influencing the final results for the stability.

Currently the breaking of waves at the location of the reefs is not taken into account. If the waves however break at the location of the reefs, this could cause an increase in the forces working on the reefs.

#### **SWAN 1D**

In the usage of SWAN 1D in this thesis, there were no possibilities to calibrate the model, since there is no nearshore wave data available. This lack of nearshore data caused the SWAN results to be unvalidatable.

#### **Structure coefficients**

The current drag and lift coefficients of the structures are not perfectly calibrated. A sensitivity analysis for the drag coefficient has been executed, but this gives no real physical parameters as a result. Also the presence of corals growing on the structures not taken into account into the stability model. The corals will however cause a higher area subjected to the water flow and could cause an increase in the drag coefficient. The influence of the use of more cubes in rows on the projected area projected to the water flow is still doubtful. The calculations in appendix A are estimations of the flow, not physically validated values. The bottom friction coefficient is determined by literature research, but the ocean bottom at the location of the reefs is not a usual bottom, since the presence of loose coral rubble and algae growing on the rubble. This could cause a lower bottom friction coefficient.

Possible imperfections during the construction of the structures are not taken into account, but are probably present due to the simple manual construction methods. Imperfections in the concrete molding could cause holes and cracks in the structures. This could lead to higher drag force values.

### 5.2 Evaluation of results

The model results seems to be a realistic result of this thesis. The original configuration became unstable during the storm in January 2023 and was stable during the storm in January 2022 according to the model. By adding more Cube L's to the configuration, the gravitational force increased. Therefore the bottom friction will increase as well. Also the addition of the Cube S and Bricks results in an increase of weight and bottom friction. It was possible to validate the model due to the availability of storm data during the life time of the reefs, causing the results to be more reliable.

## 6 Conclusion: final configuration selection

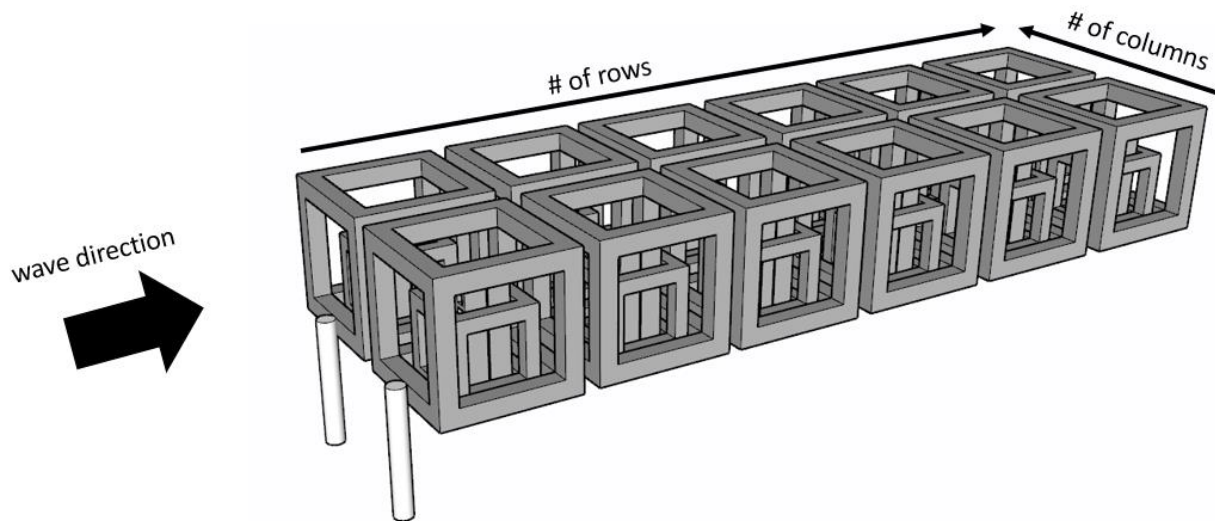


Figure 6-1: Final configuration.

The results obtained in chapter 4 lead to the configuration as shown in Figure 6-1. The configuration consists of 2 columns and 6 rows of Cube L, filled with both the Cube S and the Bricks. The wave direction is perpendicular to the shore, the configuration is therefore also installed perpendicular to the shore.

The objective of this thesis was stated as follows:

*Evaluate and optimize a simple configuration of cube framework artificial reef structures, for reefs located at the north east shore of Bali, Indonesia, which remains stable during storm conditions.*

To complete the objective, answers were needed for the succeeding sub questions:

- What are the hydraulic design storm conditions at the north east coast of Bali, Indonesia?
- What combination of artificial reef structures result in a stable configuration during the design storm conditions?

For the first sub question, the nearshore design hydraulic conditions of were obtained. These design conditions are displayed in Table 6-1. For the second sub question a force equilibrium model was created, resulting in a configuration as shown in Figure 6-1.

Parameter	Value
$H_s$	0.98 [m]
$T_p$	6.85 [s]
$L$	35.77 [m]
$d$	3.03 [m]

Table 6-1: Obtained nearshore hydraulic design conditions.

## 7 Recommendations

### **Data collection**

To increase the accuracy of the offshore to nearshore wave transformation, it is recommended to add sensors to measure water pressure, to monitor the nearshore water level, wave height and wave period. This data can be used to validate and calibrate the SWAN model.

### **Wave flume research**

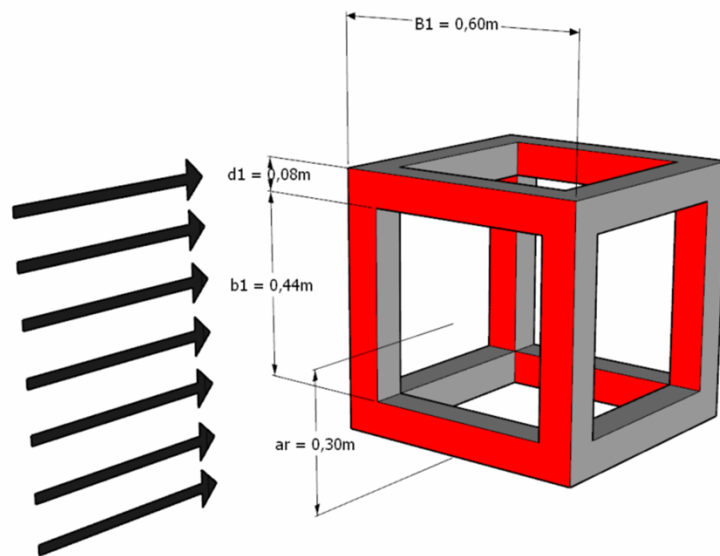
The structure coefficients (drag and lift) can be determined by executing wave flume tests. The structure coefficients are needed to optimize the stability model. Also the presence of corals on the structures should be simulated, probably causing an increase in drag.

### **Structure adjustments**

The force with the most influence on the horizontal stability is the drag force. It is possible to reduce the drag force by using rounded corners on the structures, lowering the drag coefficient. The bottom friction force could be increased by using concrete with a higher specific weight. This can be done by using a less porous aggregate mix.

It is recommended to reinstall the Cube S and Bricks in the Cube L structures. These parts have a positive effect on the stability due to their weight. They have to be firmly connected to the Cube L. It is recommended to look into possibilities to create stiffer connections between the different cubes and bricks.

Appendix A: Calculation of area normal projected to flow  
**Cube L in front row**



$$S_1 = 2B_1d_1 + 6b_1d_1 = 0,3072 [m^2]$$

$$a_r = \frac{B_1}{2}$$

In which:

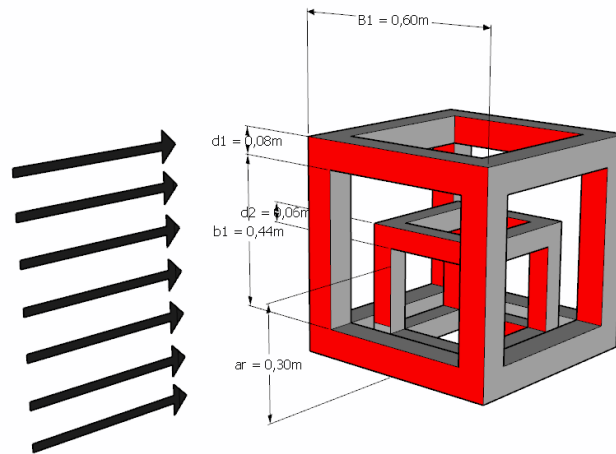
$S_1$ : projected area of single Cube L normal to the force direction [ $m^2$ ]

$B_1$ : total width Cube L = 0,6 [m]

$b_1$ : inside width Cube L = 0,44 [m]

$d_1$ : rod width Cube L = 0,08 [m]

### Cube L with Cube S in front row



$$S_2 = 2B_1d_1 + 5b_1d_1 + 2d_2(B_2 - d_1) + 5b_2d_2 = 0,3776 \text{ [m}^2\text{]}$$

In which:

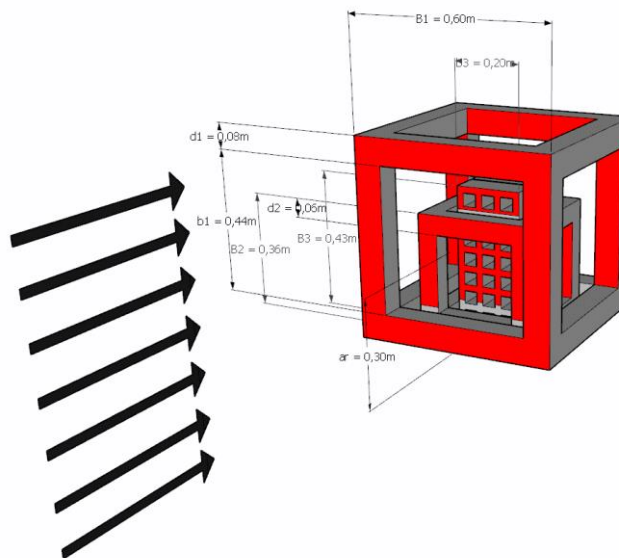
$S_2$ : projected area of Cube L with Cube S normal to the force direction [m<sup>2</sup>]

$B_2$ : total width Cube S = 0,36 [m]

$b_2$ : inside width Cube S = 0,24 [m]

$d_2$ : rod width Cube S = 0,06 [m]

### Cube L with Cube S and Bricks in front row



$$S_3 = 2B_1d_1 + 5b_1d_1 + 2d_2(B_2 - d_1) + 3b_2d_2 + (B_3 - d_1 - d_2)b_3 = 0,4068 \text{ [m}^2\text{]}$$

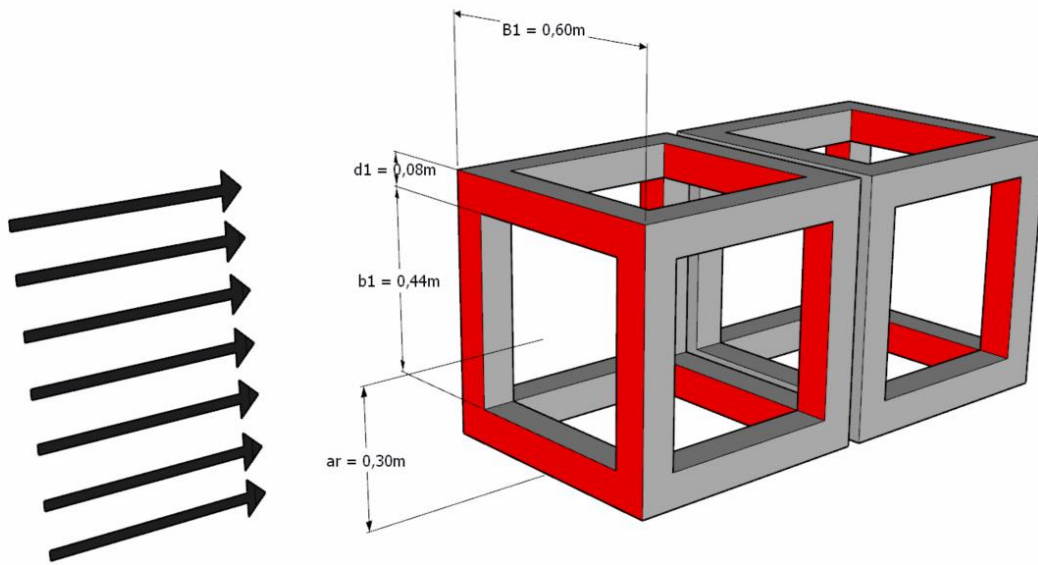
In which:

$S_3$ : projected area of single Cube L with Cube S and Bricks normal to the force direction [m<sup>2</sup>]

$B_3$ : height Brick = 0,43 [m]

$b_3$ : width Brick = 0,20 [m]

**Cube L behind other row**

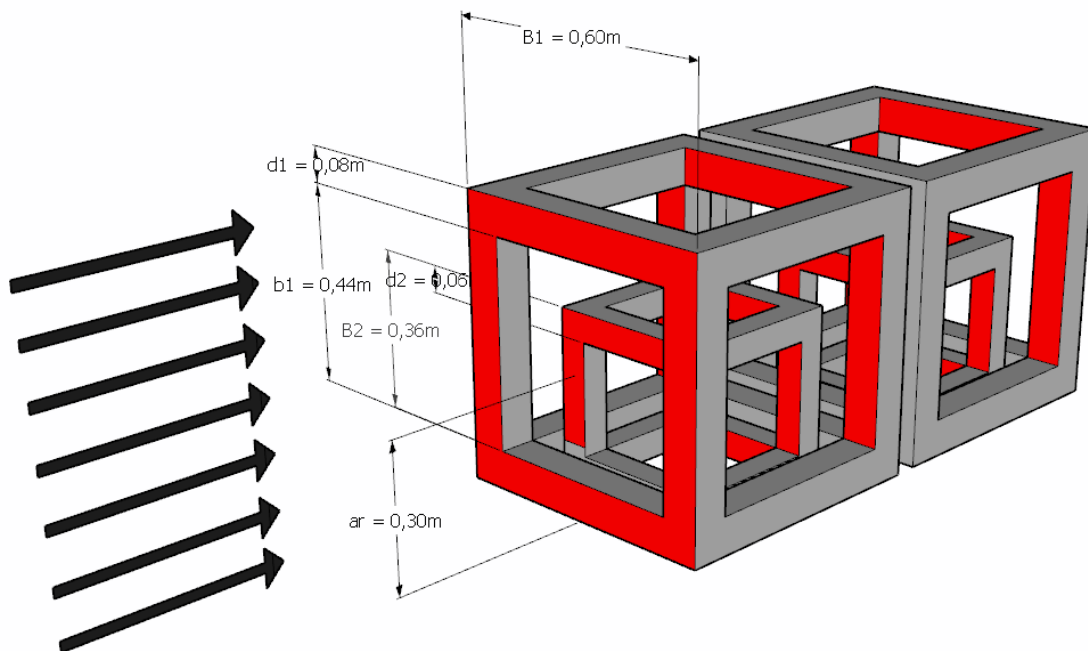


$$S_4 = 4b_1d_1 = 0,1408 \text{ [m}^2\text{]}$$

In which:

$S_4$ : projected area of single Cube L behind other cube, normal to the force direction [m<sup>2</sup>]

**Cube L with Cube S behind other row**

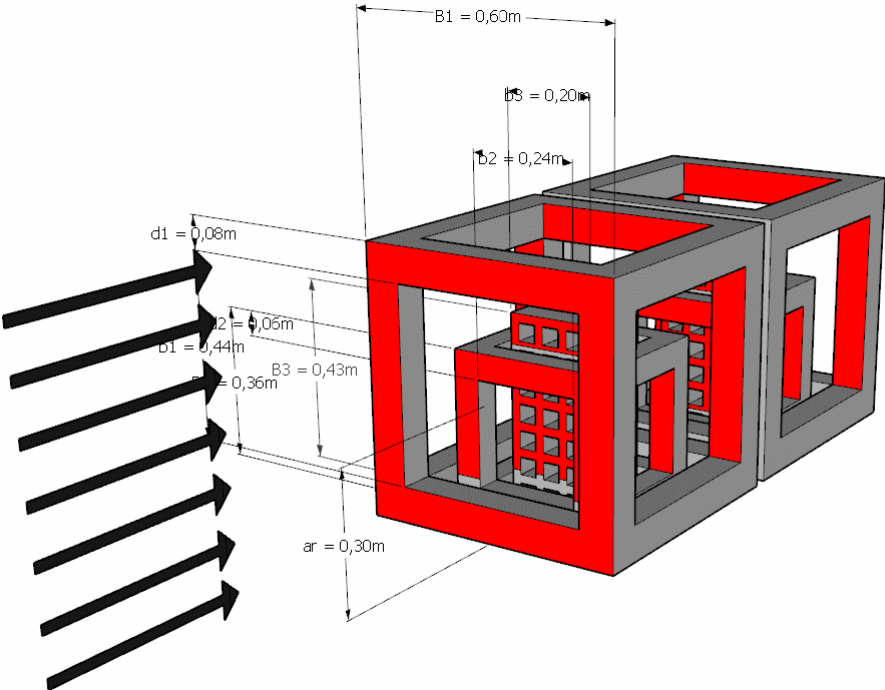


$$S_5 = 3b_1d_1 + 2d_2(B_2 - d_1) + 5b_2d_2 = 0,2112 \text{ [m}^2\text{]}$$

In which:

$S_5$ : projected area of Cube L with Cube S behind other cube, normal to the force direction [m<sup>2</sup>]

**Cube L with Cube S and Bricks behind other row**

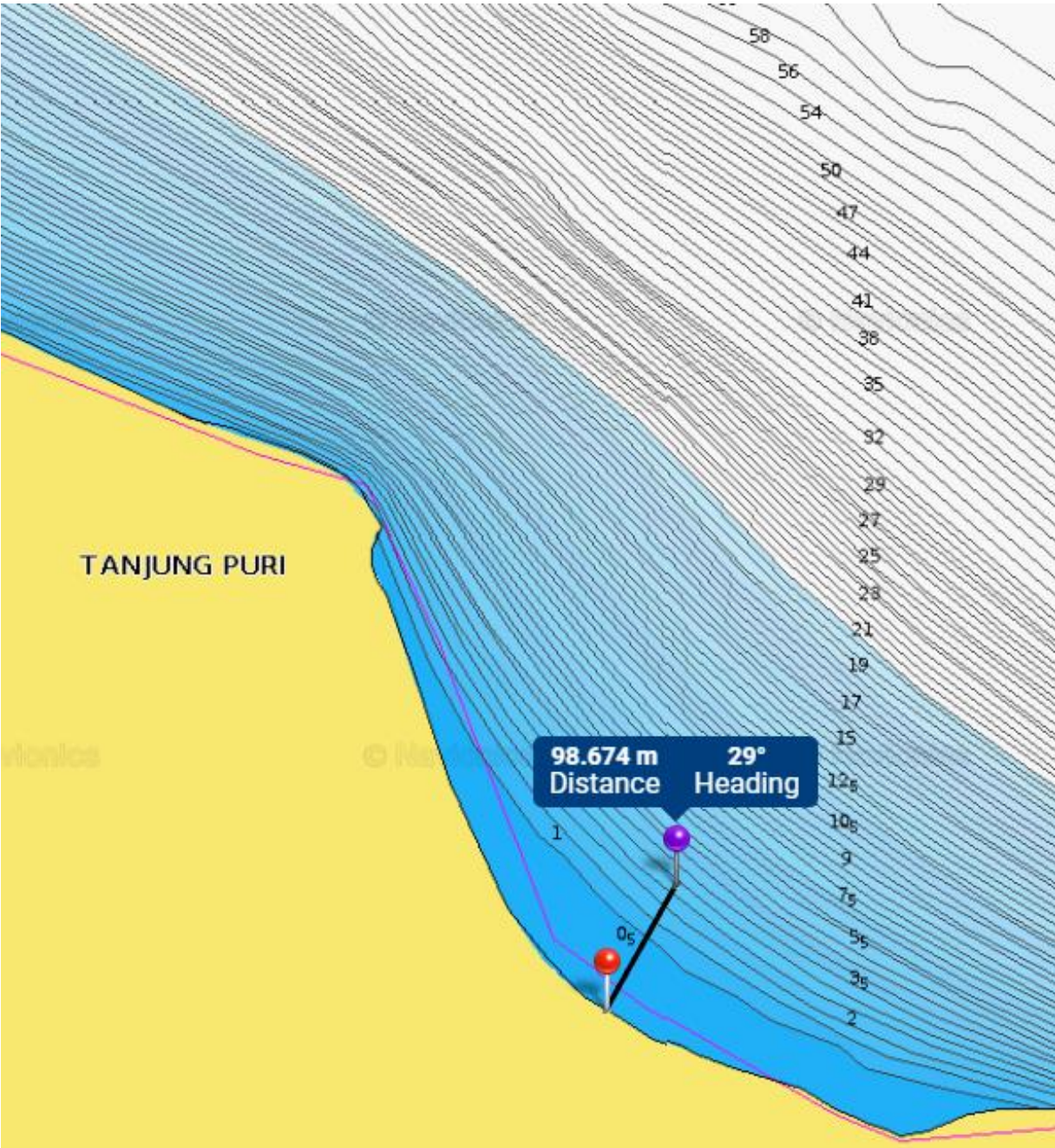


$$S_6 = 3b_1d_1 + 2d_2(B_2 - d_1) + 3b_2d_2 + (B_3 - d_1 - d_2)b_3 = 0,2404 [m^2]$$

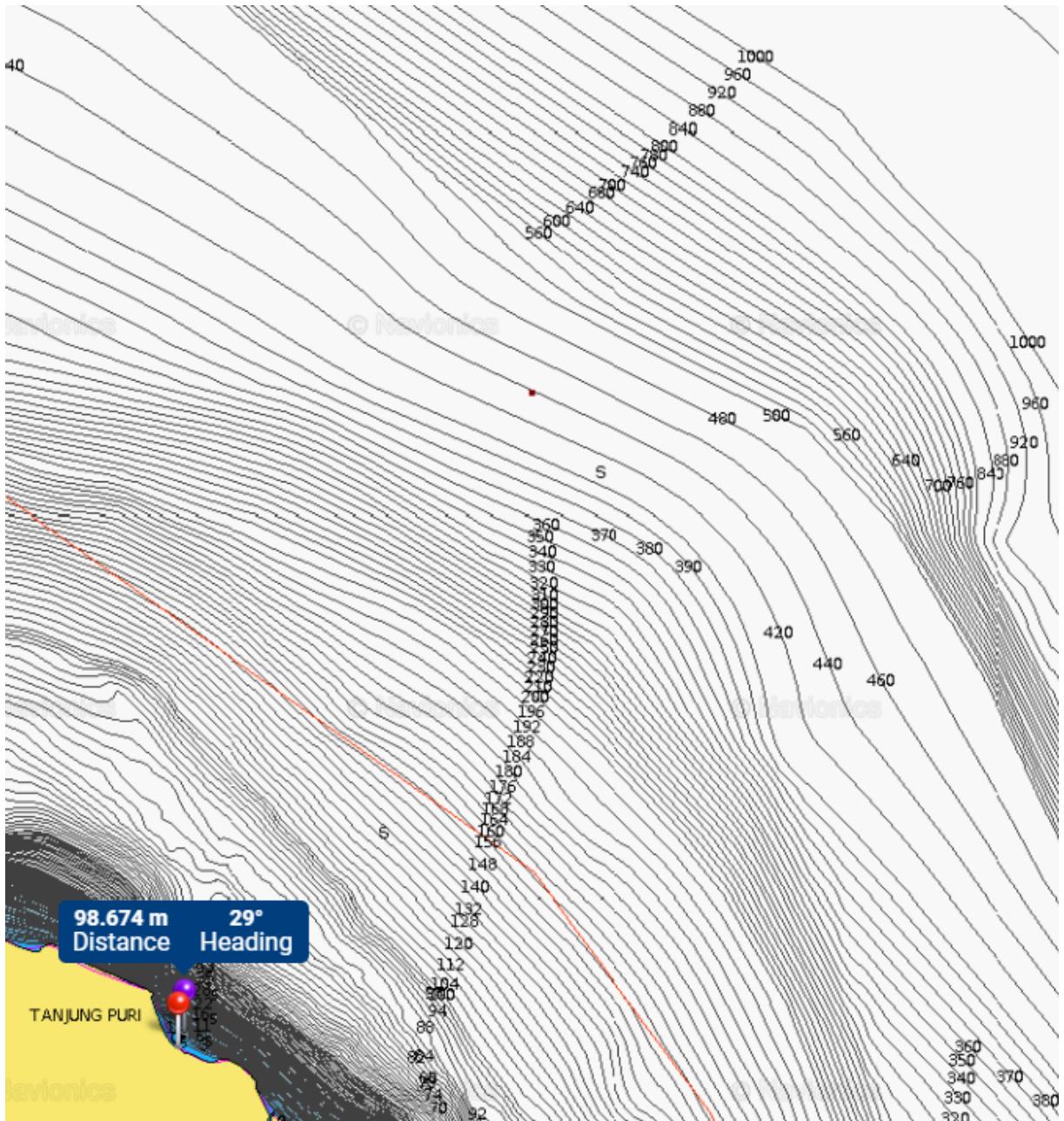
In which:

$S_6$ : projected area of Cube L behind other cube with Cube S and Bricks normal to the force direction [ $m^2$ ]

Appendix B: Sonar map of Navionics (Navionics, 2023)



(Navionics, 2023)



(Navionics, 2023)

## Appendix C: SWAN 1D model

```
$*****HEADING*****
$
PROJECT 'Bali nearshore' '1'
$
$
$*****MODEL INPUT*****
SET 1 90 0.05 200 2
SET NAUTICAL
MODE STAT ONED
COORDINATES SPHERICAL
$-----
CGRID 115.67 -8.34 11.71 0.143 0 99 0 CIRCLE 36 0.03 3 99
$-----
INPGRID WLEVEL 115.67 -8.34 11.71 99 0 0.00072 0
INPGRID BOTTOM 115.67 -8.34 11.71 99 0 0.00072 0
$-----
READINP BOTTOM -1 'bottomfit.dep' 1 FREE
$-----
BOUND SHAPESPEC JONSWAP 3.3 PEAK
$-----
BOUNDSPEC SIDE NORTHEAST CONSTANT PAR 2.5 7 150
$-----
$INITIAL PAR 2.5 7 150
$-----
GEN3 JANSSEN
BREAKING
FRICTION
DIFFRACTION
$-----
QUAD iquad=1
$-----
NUM STOPC 0.005 0.01 0.005 99.5 STAT 100 0.01
$***** OUTPUT REQUESTS *****
CURVE 'LINE1' 115.67 -8.34 1000 115.7 -8.2
TABLE 'LINE1' HEAD 'Bali_output.tab' XP YP HS RTPEAK DEPTH LWAVP DIR
COMPUTE
STOP
```

## Appendix D: Python code for stability model

```
In [1]: import numpy as np
import matplotlib.pyplot as plt
```

```
In [2]: # hs, tp, d, l
s2022 = [0.66, 5.96, 3.0, 30.66] # nearshore data of Jan 2022 storm
s2023 = [0.75, 7.18, 3.0, 35.77] # nearshore data of Jan 2023 storm
sdesign = [0.98, 6.85, 3.0, 35.77] # nearshore data of design storm
```

```
In [3]: #dimensions of structure
def VS(col, row, s, b):
    v1 = 0.037888 # volume of Cube L
    v2 = 0.012096 # volume of Cube S
    v3 = 0.005425 # volume of single Brick
    s1 = 0.3072 # area subjected to flow front row Cube L
    s2 = 0.3776 # area subjected to flow front row Cube L with Cube S
    s3 = 0.4068 # area subjected to flow front row Cube L with Cube S and Bricks
    s4 = 0.1408 # area subjected to flow other rows Cube L
    s5 = 0.2112 # area subjected to flow other rows Cube L with Cube S
    s6 = 0.2404 # area subjected to flow other rows Cube L with Cube S and Bricks
    V = col*row*v1 + col*row*s*v2 + col*row*b*v3*2
    S = np.max([s1*col+(row-1)*s4*col, s*(s2*col+(row-1)*s5*col) ,b*(s3*col+(row-1)*s6*col)])
    return V, S
```

```
In [4]: #forces on structure, returns horizontal and moment equilibrium
# s = 2116.4
# b = 1935.5
def forces(hs, tp, d, l, Cd, Cl, V, S, mu, row):
    rhow = 1025 # density of water
    rhos = 2100 # density of structure
    g = 9.81
    ar = 0.3 # vertical moment arm
    hd = np.min([np.math.sqrt(-0.5*np.math.log(-np.math.log(0.99)/(60*60*2/tp)))*hs,d*0.6]) # design wave height
    k = (2*3.1415)/l # wave number
    u = (3.1415*hd*np.math.cosh((k*0.6)))/(tp*np.math.sinh(d*k)) # orbital velocity of upper part of structure
    drag = 0.5*Cd*rhow*S*u**2 # drag force
    grav = (rhos-rhow)*g*V # gravitational force
    lift = 0.5*Cl*rhow*S*u**2 # lift force
    bottom = mu*(grav-lift) # bottom friction force
    hor = bottom-drag # horizontal force equilibrium
    m = -ar* drag-lift*row*0.6*0.5 + grav*row*0.6*0.5 # moment equilibrium
    return hor, m, drag, hd, u
```

```
In [15]: #define configuration and calculate force equilibrium
col = 2 # number of columns of configuration
row = 4 # number of row of configuration
Cd = 1.1 # drag coefficient
Cl = 0.2 # lift coefficient
mu = 0.6 # bottom friction coefficient
V, S = VS(col,row,1,1) # volume and area of total configuration
hs, tp, d, l = s2023
forces(hs, tp, d, l, Cd, Cl, V, S, mu, row)
```

## Literature

- Diringer, V. (2021). *Determining the efficiency of artificial reefs in different settings and the best parameters for their success* Universiteit Leiden].
- Elger, D. F., LeBret, B. A., Crowe, C. T., & Roberson, J. A. (2020). *Engineering fluid mechanics*. John Wiley & Sons.
- GEBCO. (2023). *GEBCO 2023 Grid*. <https://doi.org/10.5285/f98b053b-0cbc-6c23-e053-6c86abc0af7b>
- Google. (2023). *Google Maps*. Retrieved 27-04 from <https://www.google.nl/maps/@-8.3715788,115.1354099,140350m/data=!3m1!1e3?hl=nl>
- Hampton-Smith, M., Bower, D. S., & Mika, S. (2021). A review of the current global status of blast fishing: Causes, implications and solutions. *Biological Conservation*, 262, 109307.
- Hersbach, H., Bell, B., Berrisford, P., Biavati, G., Horányi, A., Muñoz Sabater, J., Nicolas, J., Peubey, C., Radu, R., Rozum, I., Schepers, D., Simmons, A., Soci, C., Dee, D., & Thépaut, J.-N. (2023). *ERA5 hourly data on single levels from 1940 to present*. <https://doi.org/10.24381/cds.adbb2d47>
- Hoerner, S. F. (1965). *Fluid-Dynamic Drag : Practical Information on Aerodynamic Drag and Hydrodynamic Resistance* (2 ed.).
- Jonkman, S. N., Steenbergen, R. D. J. M., Morales-N´apoles, O., Vrouwenvelder, A. C. W. M., & Vrijling, J. K. (2017). Probabilistic design: Risk and reliability analysis in civil engineering lecture notes cie4130. In.
- Kamphuis, J. W. (2000). *Introduction to Coastal Engineering and Management* (Vol. 16). World Scientific Publishing Co. Pte. Ltd.
- Longuet-Higgins, M. S. (1952). On the statistical distribution of the heights of sea waves. *JOURNAL OF MARINE RESEARCH*, XI, 245-266.
- Massel, S. R. (1996). On the largest wave height in water of constant depth. *Ocean Engineering*, 23(7), 553-573.
- Navionics. (2023). *Sonar Chart*. [https://webapp.navionics.com/?lang=en#boating@13&key=va%7Dq%40%7B~\\_aU](https://webapp.navionics.com/?lang=en#boating@13&key=va%7Dq%40%7B~_aU)
- Reynolds, O. (1883). XXIX. An experimental investigation of the circumstances which determine whether the motion of water shall be direct or sinuous, and of the law of resistance in parallel channels. *Philosophical Transactions of the Royal Society of London*, 174, 935-982. <https://doi.org/10.1098/rstl.1883.0029>
- Siderius, E. (2022). *Droppable Oyster Brood Stock Structure* TU Delft].
- tidechart.com. (2023). *Abang tide times and tide charts for this week*. tideschart.com. Retrieved 12-06 from <https://www.tideschart.com/Indonesia/Bali/Abang/Weekly/>
- Tito, C. K., & Ampou, E. E. (2019, Sep 04). Coral reefs ecosystem degradation at Nusa Penida, Bali. *IOP Conference Series-Earth and Environmental Science* [3rd international conference on marine science (icms) 2019 - towards sustainable marine resources and environment]. 3rd International Conference on Marine Science (ICMS) - Towards Sustainable Marine Resources and Environment, Bogor City, INDONESIA.
- Wieselsberger, C., & United, S. (1922). *Further information on the laws of fluid resistance*. National Advisory Committee for Aeronautics. <https://purl.fdlp.gov/GPO/gpo134251>